Algorithm for converting full-parallax holograms to horizontal-parallax-only holograms

Taegeun Kim,[1,*] You Seok Kim,[1] Won Sun Kim,[2] and Ting-Chung Poon[3]

[1]*Department of Optical Engineering, Sejong University, 98 Kunja-dong, Kwangjin-gu, Seoul 134-747, Korea*
[2]*Meere Company, 285-15 Jeongmun-ri, Yangnam-myeon, Hwaseng-si, Gyeonggi-do 445-933, Korea*
[3]*Department of Electrical and Computer Engineering, Virginia Tech, Blacksburg, Virginia 24061, USA*
**Corresponding author: takim@sejong.ac.kr*

Received January 6, 2009; revised February 20, 2009; accepted February 25, 2009;
posted March 13, 2009 (Doc. ID 106014); published April 8, 2009

We propose an algorithm that converts a full-parallax hologram to a horizontal-parallax-only (HPO) hologram for 3D display. We first record a full-parallax hologram of an object. Subsequently, we filter the hologram with a Gaussian low-pass filter and a fringe-matched filter along the vertical direction. The final filtered output becomes an HPO hologram. To the best of our knowledge, this is the first algorithm proposed for converting full-parallax holographic information to HPO-holographic information. © 2009 Optical Society of America

OCIS codes: 090.1995, 090.2870.

A horizontal-parallax-only (HPO) hologram has been proposed as an excellent way to reduce the required amount of data for 3D display [1,2]. While HPO optical scanning holography (OSH) has been suggested as an electro-optical technique that actually can record the HPO-holographic information of a 3D object [3,4], a digital technique that synthesizes a modified HPO hologram using multiple viewpoint recordings of an object using a CCD camera has shown the recording of holographic data containing the horizontal-parallax effect [5].

We propose an algorithm that converts a full-parallax hologram to an HPO hologram by using Gaussian low-pass filtering and fringe-matched filtering. Although a full-parallax hologram of a 3D object can be considered as a collection of 2D Fresnel zone plates (FZPs), an HPO hologram is a collection of 1D FZPs [4]. Figures 1(a) and 1(b) show a 2D FZP and an asymmetrical FZP, respectively. The asymmetrical FZP shown in Fig. 1(b) illustrates an approximation to a line or 1D FZP by masking a slit along the x direction. Note that the asymmetrical FZP still has curvature within its vertical extent if the slit size is not small enough, and hence it will generate aberration upon reconstruction of the hologram.

We first propose to use a Gaussian low-pass filter along the y direction on the spectrum of the full-parallax hologram to create an asymmetrical FZP. Gaussian low-pass filtering along the vertical direction removes the high-frequency components of the object along the vertical direction. This makes it possible to reduce the amount of data by sacrificing the vertical parallax without losing the horizontal parallax. The filtered output becomes a hologram in which the object is encoded by an asymmetrical FZP. To remove the curvature along the vertical direction of the asymmetrical FZP, we further propose a fringe-matched filter, which compensates the curvature of the Gaussian low-pass filtered hologram along the vertical direction and gives an exact HPO hologram as an output [1,2]. Figure 2 shows the optical scanning holography (OSH) setup that records the full-parallax complex hologram of an object [6]. OSH is a form of digital holography that is composed of a Mach–Zehnder interferometer and an electronic processing unit. The interferometer includes acousto-optical frequency shifters (AOFS1 and AOFS2) and beam expanders (BE1 and BE2) with a focusing lens (L1). While beam expander BE1 and lens L1 generate a spherical wave at a temporal frequency of $\varpi_o+\Omega+\Delta\Omega$ away from beam splitter BS2, where ϖ_o is the frequency of the laser and $\Omega+\Delta\Omega$ is the operating frequency of the frequency shifter AOFS1, beam expander BE2 generates a plane wave at a temporal frequency of $\varpi_o+\Omega$ toward BS2 as AOFS2 operates at frequency Ω. The spherical wave and the plane wave combined at beam splitter BS2 then generate a so-called time-dependent FZP (TD-FZP) onto the 3D object, $I_o(x,y,z)$. The TD-FZP is modulated in time by the frequency difference $\Delta\Omega$ between AOFS1 and AOFS2. The AOFS1,2 are driven by 40 and 40.01 MHz, respectively, in the experiment and hence $\Delta\Omega/2\pi=10$ kHz. The TD-FZP scans the object shown in Fig. 2, and the transmitted light through the object is spatially integrated by the collecting lens (L2). The spatially integrated light is then converted into electric current by the photodetector (PD). The electric current is subsequently demodulated by an in- and quadrature-phase demodulator, and the demodulated signals are stored in a digital computer to eventually generate a full-parallax complex hologram given by [4,6]

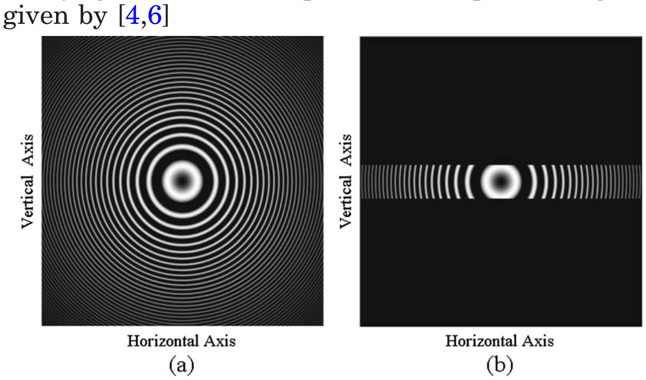

Fig. 1. (a) Full-parallax FZP, (b) asymmetrical FZP.

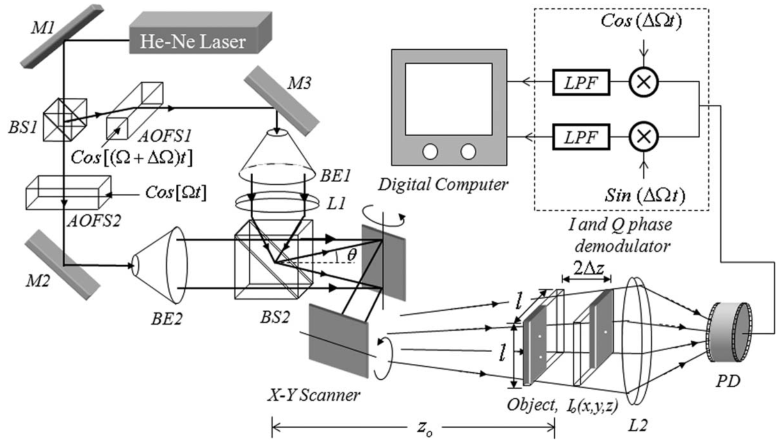

Fig. 2. Optical scanning holographic recording: M, mirrors; AOFS1,2, acousto-optical frequency shifters; BS1,2, beam splitters; BE1,2, beam expanders; L1, focusing lens; θ, half-cone angle subtended by the FZP; L2, collecting lens; PD, photodetector; $\otimes$, electronic multiplier; LPF, low-pass filter).

$$H_{full}(x,y) = \int_{z_o-\Delta z}^{z_o+\Delta z} I_o(x,y,z) \otimes \frac{j}{\lambda z} \times \exp\left\{\left(\frac{-\pi}{\mathrm{NA}^2 z^2} + j\frac{\pi}{\lambda z}\right)(x^2+y^2)\right\} \mathrm{d}z, \tag{1}$$

where NA represents the numerical aperture defined as the sine of the half-cone angle subtended by the TD-FZP, λ is the wavelength of the laser, z_o is the depth location of the object, $2\Delta z$ is the depth range of the object as shown in Fig. 2, and the symbol $\otimes$ denotes 2D convolution. Our goal is to convert the full-parallax hologram, $H_{full}(x,y)$, into a HPO hologram. The spectrum of the hologram is given by

$$\boldsymbol{H_{full}}(k_x,k_y) = F\{H_{full}(x,y)\} = \int_{z_o-\Delta z}^{z_o+\Delta z} \boldsymbol{I}_o(k_x,k_y,z) \times \exp\left\{\left[-\frac{1}{4\pi}\left(\frac{\lambda}{\mathrm{NA}}\right)^2 + j\frac{\lambda z}{4\pi}\right](k_x^2+k_y^2)\right\}\mathrm{d}z, \tag{2}$$

where $F\{.\}$ represents Fourier transformation with (k_x,k_y) denoting spatial frequencies. We now apply a Gaussian low-pass filter along the vertical direction, $\boldsymbol{G_{low\text{-}pass}}(k_x,k_y) = \exp[-1/4\pi(\lambda/\mathrm{NA}_g)^2 k_y^2]$, to the full-parallax hologram's spectrum given by Eq. (2), where NA_g is a parameter that determines the cutoff frequency of the Gaussian low-pass filter. The filtered spectrum is then given by

$$\boldsymbol{H_{asym\ FZP}}(k_x,k_y) = \boldsymbol{H_{full}}(k_x,k_y)\boldsymbol{G_{low\text{-}pass}}(k_x,k_y) = \int_{z_o-\Delta z}^{z_o+\Delta z} \boldsymbol{I}_o(k_x,k_y,z) \times \exp\left[\left\{-\frac{1}{4\pi}\left(\frac{\lambda}{\mathrm{NA}}\right)^2 + j\frac{\lambda z}{4\pi}\right\}k_x^2 + \left\{-\frac{1}{4\pi}\left(\frac{\lambda}{\mathrm{NA}_{lp}}\right)^2 + j\frac{\lambda z}{4\pi}\right\}k_y^2\right]\mathrm{d}z, \tag{3}$$

where $\mathrm{NA}_{lp} = \mathrm{NA}_g \mathrm{NA}/\sqrt{\mathrm{NA}^2+\mathrm{NA}_g^2}$ is the NA of the FZP along the vertical direction. Note that the Gaussian low-pass filtered hologram is a hologram in which the object's cross-sectional images are encoded with the asymmetrical FZP. As discussed earlier, the asymmetric FZP has curvature along the vertical direction. To remove the curvature, we propose a fringe-matched filter, $\boldsymbol{F_{fm}}(k_x,k_y) = \exp[-j\lambda z_o/4\pi k_y^2]$, that compensates the curvature along the vertical direction, where z_0 is the depth location of the object. Hence the fringe-adjusted filtered output becomes

$$\boldsymbol{H_{HPO}}(k_x,k_y) = \boldsymbol{H_{asym\ FZP}}(k_x,k_y)\boldsymbol{F_{fm}}(k_x,k_y) = \int_{z_o-\Delta z}^{z_o+\Delta z} \boldsymbol{I}_o(k_x,k_y,z) \times \exp\left[\left\{-\frac{1}{4\pi}\left(\frac{\lambda}{\mathrm{NA}}\right)^2 + j\frac{\lambda z}{4\pi}\right\}k_x^2 + \left\{-\frac{1}{4\pi}\left(\frac{\lambda}{\mathrm{NA}_{lp}}\right)^2 + j\frac{\lambda(z-z_o)}{4\pi}\right\}k_y^2\right]\mathrm{d}z. \tag{4}$$

The HPO hologram in space domain is given by $H_{HPO}(x,y) = F^{-1}\{\boldsymbol{H_{HPO}}(k_x,k_y)\}$, where $F^{-1}\{.\}$ represents the inverse Fourier transformation. Now, in the

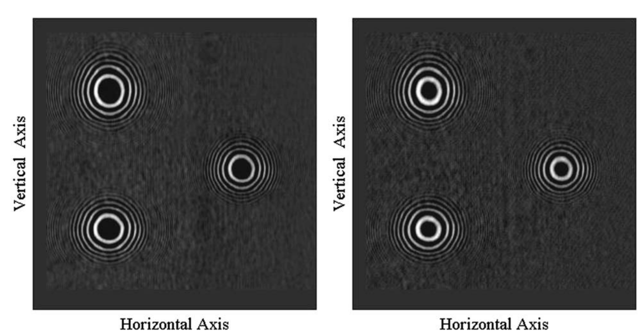

(a) (b)

Fig. 3. (a) Real part of the full-parallax hologram (1.8 cm by 1.8 cm), (b) imaginary part of the full-parallax hologram (1.8 cm by 1.8 cm).

case that the depth range of the object ($2\Delta z$) is smaller than the in-focus range of the line FZP along the vertical direction ($2\Delta z_{ver\_dir}=2\lambda/(\mathrm{NA}_{lp}^2)$), i.e., $\Delta z \leqslant \Delta z_{ver\_dir}$, which is usually true when we synthesize an HPO hologram for 3D display, $z \approx z_o$ within the range of the object depth along the y direction, and hence the last term of the exponential function become zero, i.e., $\lambda(z-z_o)/4\pi \approx 0$. Equation (4) then becomes

$$\boldsymbol{H_{HPO}}(k_x,k_y) = \int_{z_o-\Delta z}^{z_o+\Delta z} I_o(k_x,k_y,z)\exp\left[\left\{-\frac{1}{4\pi}\left(\frac{\lambda}{\mathrm{NA}}\right)^2 + j\frac{\lambda z}{4\pi}\right\}k_x^2 + \left\{-\frac{1}{4\pi}\left(\frac{\lambda}{\mathrm{NA}_{lp}}\right)^2\right\}k_y^2\right]\mathrm{d}z, \quad (5)$$

and its spatial domain expression is

$$H_{HPO}(x,y) = F^{-1}\{\boldsymbol{H_{HPO}}(k_x,k_y)\} = \int_{z_o-\Delta z}^{z_o+\Delta z} \boldsymbol{I}_o(x,y,z) \otimes \frac{j}{\lambda z} \times\exp\left[-\left(\frac{\pi}{\mathrm{NA}^2 z^2} + j\frac{\pi}{\lambda z}\right)x^2 - \frac{\pi}{\mathrm{NA}_{lp}^2 z^2}y^2\right]\mathrm{d}z, \quad (6)$$

which is the exact expression of the HPO hologram of a computer-generated HPO hologram [1,2,4]. The data amount that is reduced by converting a full-parallax hologram to an HPO hologram can be determined as follows. When we represent a hologram on a spatial light modulator (SLM), the pixel pitch, Δl, required to represent a FZP without aliasing is given by $\Delta l \leqslant \lambda/2\mathrm{NA}$ [3]. The required pixel pitch of the HPO hologram along the horizontal and vertical directions are given by $\Delta l_{hor} \leqslant \lambda/2\mathrm{NA}$ and $\Delta l_{ver} \leqslant \lambda/2\mathrm{NA}_{lp}$, respectively. Thus, when we represent the HPO hologram on an SLM with the size of $l \times l$, the required number of samples (or resolvable pixels) that represents the HPO hologram is given by $N_{HPO} = (l/\Delta l_{hor}) \times (l/\Delta l_{ver})$. However, when we represent the full parallax hologram on an SLM, the required number of samples is given by $N_{full}=(l/\Delta l_{hor})^2$. Here we define the ratio of the required numbers of samples between the HPO hologram and the full-parallax hologram as a data reduction ratio that is given by $R=N_{HPO}/N_{Full}=\mathrm{NA}_{lp}/\mathrm{NA}$. In the experiment, an object is composed of three points on two slides, as shown in Fig. 2. The depth location of the object is $z_o=87$ cm, and the distance between two slides is $2\Delta z=20$ cm. The xy scanning region of the object is $l \times l = 1.8\ \mathrm{cm} \times 1.8\ \mathrm{cm}$. The diameter of the points is 200 μm. The diameter of the collimated beam is $D=25$ mm, and the focal length of the lens is $f=500$ mm. Thus, the NA of the recorded full-parallax complex hologram is $\mathrm{NA} \approx D/(2f) = 0.025$. Figures 3(a) and 3(b) show the real and imaginary parts of the full-parallax complex hologram. We set the filter parameter $\mathrm{NA}_g=0.00056$. For our experiment, $\mathrm{NA}_{lp}=0.00056$, which gives the data-reduction ratio of $R=\mathrm{NA}_{lp}/\mathrm{NA}=0.022$. Also, as a check, we calculated that $\Delta z_{ver\_dir}=202\ \mathrm{cm} \geqslant \Delta z=10$ cm, which is consistent with the approximation we made earlier about synthesizing an HPO hologram. The HPO hologram, according to Eq. (6), that is converted by the proposed filtering technique is shown in Figs. 4(a) and 4(b). Here we can see that the FZP that encodes the points is a 1D or line FZP having fringes along the horizontal direction only. Figures 5(a) and 5(b) show digital reconstruction of the complex hologram. This is simply done by digitally convolving the HPO hologram, given by Eq. (6), with the free-space impulse response of light propagation at each focused location of the slides. Here we can see that the reconstructed points at each focused location are spread along the vertical direction as predicted [4]. The reconstructed image spreading along the y direction can be compensated by using a cylindrical lens to focus along the vertical direction the same as conventional HPO hologram reconstructions in computer-generated holography [1].

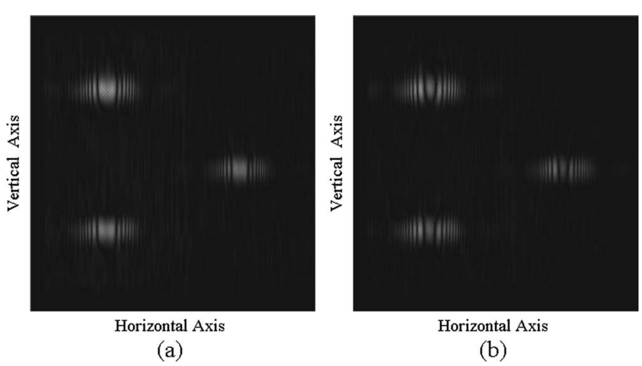

Fig. 4. (a) Real part of the HPO hologram (1.8 cm by 1.8 cm), (b) imaginary part of the HPO hologram (1.8 cm by 1.8 cm).

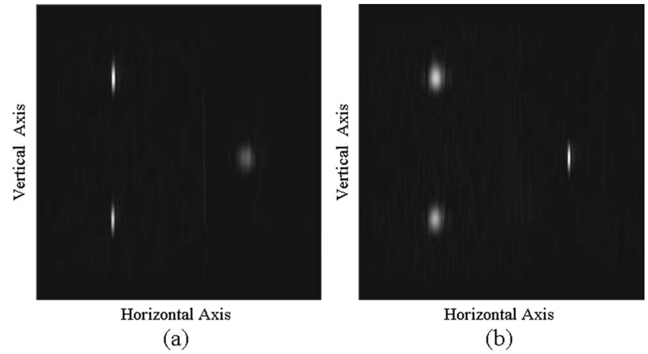

Fig. 5. (a) Reconstructed image at the front slide location (1.8 cm by 1.8 cm), (b) reconstructed image at the back slide location (1.8 cm by 1.8 cm).

References

1. P. St. Hilaire, S. A. Benton, and M. Lucente, J. Opt. Soc. Am. A **9**, 1969 (1992).
2. H. Yoshikawa and H. Taniguchi, Opt. Rev. **6**, 118 (1999).
3. T.-C. Poon, J. Soc. Inf. Disp. **3**, 12 (2002).
4. T.-C. Poon, T. Akin, G. Indebetouw, and T. Kim, Opt. Express **13**, 2427 (2005).
5. N. T. Shaked and J. Rosen, Appl. Opt. **47**, D21 (2008).
6. T.-C. Poon, T. Kim, G. Indebetouw, M. H. Wu, K. Shinoda, and Y. Suzuki, Opt. Lett. **25**, 215 (2000).